Current Control using Pulsed Current Sampling Considering Sampling Points and Sensor Positions for Single-Phase Inverter

Kensuke Suzuki, Keiji Wada
Tokyo Metropolitan University Tokyo, JAPAN
E-mail: kj-wada@tmu.ac.jp

***Abstract*—Conventional power converter circuits include two types of current sensors, one for current control and the other for overcurrent protection. Recently, research has been conducted on current sensors intended to be integrated inside power modules. These sensors are supposed to protect a power device from overcurrent. In addition, power converter circuits must implement current sensors for ac-side current control. Normally, these current sensors are used independently; thus, two types of sensors are required. However, if the sensors for protection could also undertake current control, then the sensor for current control can be eliminated. The current waveform of power devices is in the form of pulsed waveforms. Thus, a sampling technique considering sensor position and synchronous sampling is necessary. This paper proposes a control procedure for output current using current sensors integrated inside the power modules. It is clear that the relationship between the sensor position and the sampling point for unipolar-modulated single-phase inverters. The validity of the proposed method is proved through an experiment with common current sensors installed in series with the power device. In addition, it should be considered that a practical current has the frequency characteristics, so the simulation including sensor characteristics was performed. Finally, the validity of a current control method is experimentally confirmed.**

***Index Terms*—Current Control, Current sensor, Digital Control, Inverter, Sampling**

I. Introduction

Power converter circuits for motor drive and utility applications have been widely used for saving energy and realizing multi-functions. One of the common uses of these converter circuits is AC output current control. Therefore, there is considerable research for studying current control and its applications [1]-[3]. Normally, current control is applied to conventional feedback control using digital or analog circuits. To realize stable control and fast response of current control, the instantaneous current waveforms should be detected without any propagation time delay. Generally, current sensors are installed at the ac side of the converter circuit for detecting a low-frequency component such as 50/60-Hz sinusoidal current.

The principles of the current sensor for ac current detection are based on a current transformer or Hall effects, among others. There are some papers which are applying their own developed current sensor to application of power converter circuits [4]-[9]. In addition, current sensors integrated inside power modules has been proposed [10]-[13]. The purpose of the sensors is mainly for overcurrent protection in power devices. If these current sensors integrated inside the power module could be appropriately used for control, eliminating the sensor installed at the ac side is possible. As a result, miniaturization and higher-power density of the circuit will be achieved. When those sensors are used for ac-side current control, the sensing method for output current should be discussed. However, integrated current sensors can detect only pulse-shaped current waveforms. If output current can be restored from pulse-shaped current, the sensors could be used for current control. Normally, the power converter circuit has to connect to the current sensor, as shown in blue, outside the power module in Fig. 1. If current control can be realized using an integrated current sensor, no current sensor needs to be connected, as shown in Fig. 2.

To restore sinusoidal current waveforms, digital control has to be applied. In addition, both the sampling point and the switching timing should be synchronized. The current waveforms inside the power module for the inverter circuit depend on the relationship between the power devices and sensor positions. Current control for motor drive is also discussed in [14] using the developed current sensor inside the power module; however, the relationship between the sensor position and the sampling point has never discussed in detail. Especially, detecting the current waveform during narrow pulse width conditions is difficult.

This paper presents current control using pulse current detection under any pulse width operations. First, the relationship between the sensor position and the sampling point is discussed. The output current of the inverter circuit can be controlled using just one current sensor for the single-phase full-bridge inverter circuit, but the sensor position has to be changed depending on the current waveforms. Due to the sensor characteristics, controlling the output current using just one sensor is difficult. This paper proposes current control using two pulse current sensors. The experimental results will demonstrate the validity of the proposed method.

II. Pulsed Current Sampling and Sensor Position

Fig. 3 shows the circuit configuration of the full-bridge single-phase inverter, and the current sensors inside the power module are connected in series with each power device. This paper presents that output current can be controlled using these current sensors. Here, i_A denotes the current flowing into the

978-1-5386-8330-9/19/$31.00 ©2019 IEEE

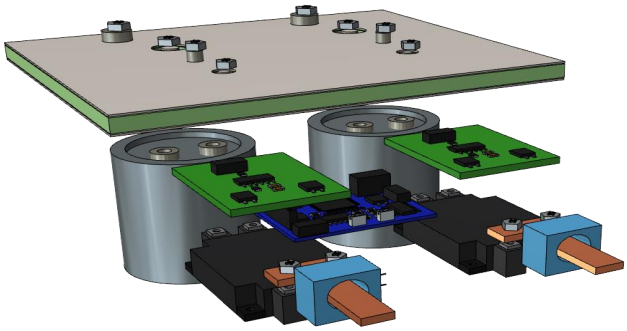

Fig. 1: Conventional circuit

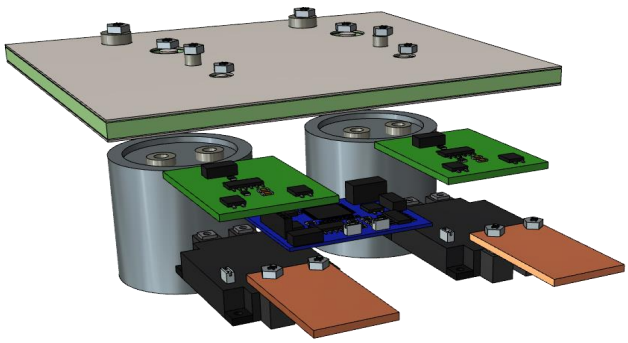

Fig. 2: Future circuit

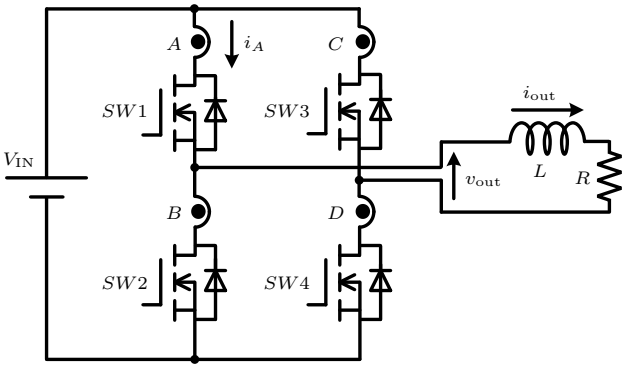

Fig. 3: Circuit configuration

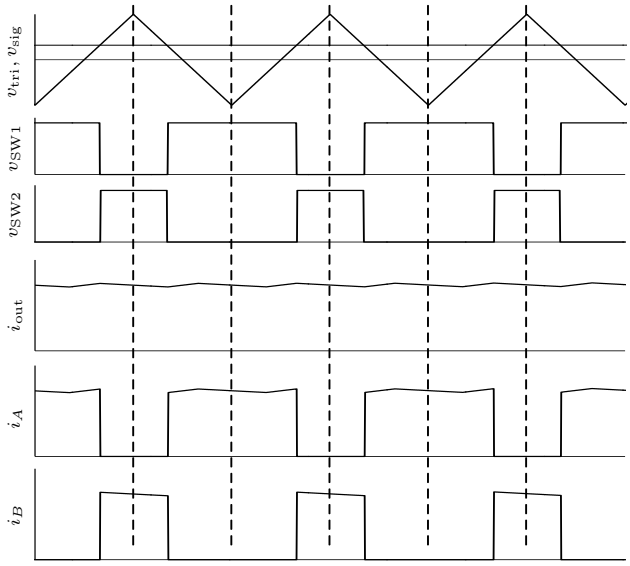

Fig. 4: Example of unipolar-modulated inverter

power device S1. The current waveform i_A becomes pulse-shape current waveform. Then, the pulsed current is sampled for detecting instantaneous current.

Table I summarizes the relationship between sensor positions and sampling points for single-phases inverter circuits. The PWM signal of the inverter circuit is generated based on a triangle carrier waveform. When using one sensor, the sampling point is decided by the sensor potions.

Fig. 4 shows the waveform of a single-phase inverter with unipolar modulation. It is confirmed that the output ac current flows into that device when the power devices are in the ON state. Thus, the instantaneous output current can be sampled using the module current sensor during the ON state of the power device. From these waveforms, the output current can be obtained by selecting appropriate sensors during the ON state. It should be noted that there is selectivity of the synchronous sampling point and power module current sensors.

III. Simulation Results

A. Simulation results using ideal current sensor

Table II shows the circuit parameters of the single-phase inverter circuit. The DC input voltage is set to 100 V. The sampling frequency becomes the same as the carrier frequency as sampling is performed once each switching cycle. The current sensor A is used for current control; hence, current sampling is conducted at the lower vertex of the carrier waveform. Fig. 5 shows the simulation result with an ideal condition when the switching frequency is set to 20 kHz. It can be confirmed that the output current is properly controlled through pulsed current sampling. Thus, only one current sensor integrated in the power module can control the output current.

B. Simulation results including practical sensor characteristics

Especially, the output characteristics of the current sensor such as delay and frequency bandwidth must be considered. Thus, simulation considering the frequency bandwidth and the output delay characteristics was performed. As a frequency characteristic of a first-order low-pass filter (LPF) is used, and the output delay characteristics of the interval period is set as delay time. Fig. 6 shows the simulation result considering sensor characteristics, and an uncontrollable region appeared.

TABLE I: Relationship between sensor positions and sampling.

Sensor position	Sampling Point	Sampling Number	Smapling Frequency
A or C	Positive Peak	1	f_{sw}
B or D	Negative Peak	1	f_{sw}
A and B (or C and D)	Both	2	$2f_{\mathrm{sw}}$
A and C (or B and D)	Both	1	f_{sw}
A, B, C, and D	All	2	$2f_{\mathrm{sw}}$

TABLE II: Simulation and Experimental Conditions

Meaning	Value
Inductance L	6.8 mH
Resistance R	21 Ω
Input Voltage V_{in}	100 V
Switching Frequency f_{sw}	10 /20 kHz
Output Frequency	50 Hz

TABLE III: Elements of the Experiment

Elements	Model number	Specification
Power Device	SPA20N60C3	650 V, 20.7 A
Current Sensor	ACS724	± 10 A, 120 kHz,
A/D Converter	LTC1412	12 bit resolution /5 V
Controller	FPGA Cyclone III	100 MHz clock

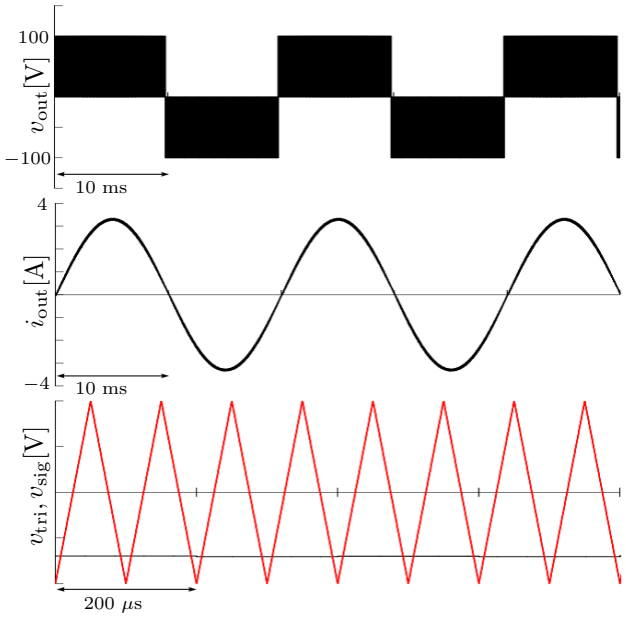

Fig. 5: Simulation result of the ideal condition

As the load resistance R is set to 21 Ω and the input voltage to 100 V, the output current became almost 5 A, as shown in the Fig. 6. As this uncontrollable region does not appear in an ideal simulation, it is considered that the output characteristic of the current sensor causes this uncontrollable region.

C. Analysis of uncontrollable region of the output current

Fig. 7 shows the PWM waveform when the uncontrollable region begins and the current flowing through the SW1, which can be detected by the sensor A. When the modulation signal V_{sig} is low, the duty ratio of the SW1 shortens. It means that the period between the switching and the current sampling also becomes short because current sampling is conducted at the lower vertex of the carrier. As the output of the sensor is affected by frequency characteristics, it is not ideal waveform, as shown in the Fig. 7. As a result, the current sensor cannot sample the current accurately. On the other hand, if the output delay time is longer than the time from the switching period to the sampling, the pulse current cannot be sampled, as shown in Fig. 7.

Owing to sensor characteristics, the uncontrollable region may appear when the ON period of the device is short. The ON period of the device is decided as per PWM. Therefore, if the sensor characteristics are already known, the available circuit conditions can be decided.

Here, the modulation rate m^* (voltage usage rate) is defined as (1).

$$m^* = \frac{i_{\mathrm{out}} * Z_{\mathrm{out}}}{V_{\mathrm{in}}} \tag{1}$$

The ratio of the minimum ON period is considered as the value obtained by subtracting the modulation rate m^* from 100% because the switches are complementary in each leg. This multiplied by the half of the carrier period becomes the minimum ON time $T_{\mathrm{ON\_min}}$. The period from the switching and sampling point can be considered as half the value of the ON time. This minimum period from the switching to the sampling must be longer than the output delay T_{delay}; otherwise, it causes the uncontrollable region of the output current. Therefore, the minimum condition of the safe operation without considering the frequency characteristics can be expressed as (2).

$$\frac{T_{\mathrm{ON\_min}}}{2} = (1 - m^*)\frac{T_{\mathrm{carrier}}}{2}\frac{1}{2} > T_{\mathrm{delay}} \tag{2}$$

Then, the following modulation ratio condition is given.

$$m^* < 1 - \frac{4T_{\mathrm{delay}}}{T_{\mathrm{carrier}}} \tag{3}$$

To obtain the correct current value of the output current, the frequency characteristics of the current sensor should be taken into account. To consider the frequency characteristics as first-order LPF, the transfer function is given by

$$\frac{Y(s)}{X(s)} = \frac{1/T_{\mathrm{fil}}}{s + 1/T_{\mathrm{fil}}} \tag{4}$$

where $X(s)$ and $Y(s)$ denote the input and output signals of the filter, respectively. Here, T_{fil} denotes the time constant

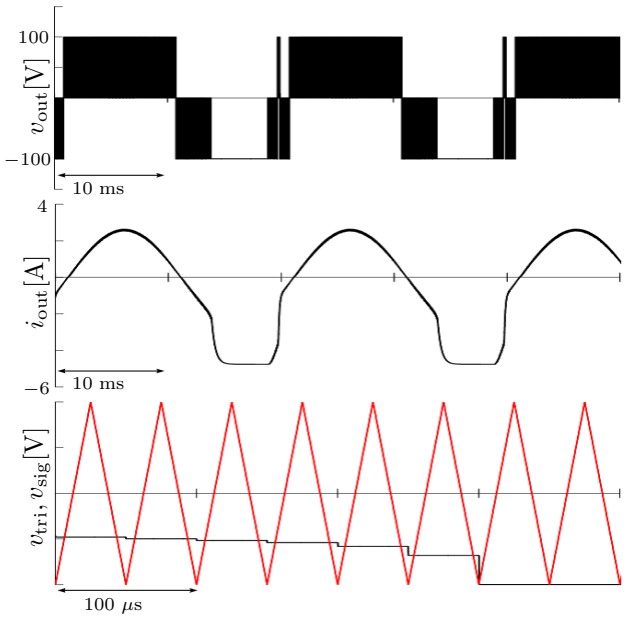

Fig. 6: Simulation result considering the practical condition

value, related to the cut-off frequency. As the input signal of the current sensor is pulsed current, it can be approximated to a step input. The step response ($X(s) = 1/s$) in the time domain is obtained with (5).

$$y(t) = 1 - e^{\frac{-t}{T_{\mathrm{fil}}}} \tag{5}$$

(5) denotes that how much time is needed for the output of the filter to become the demanded value. Therefore, if once the ratio of the output value to the input value is set, then the time T_{response} required to reach that output value could be calculated by (6).

$$T_{\mathrm{response}} > -T_{\mathrm{fil}} \ln(1 - D) \tag{6}$$

Here, D represents the duty ratio of the output value. The frequency characteristics can be included in the condition of the controllable operation region by adding the response time T_{response} to T_{delay}.

IV. Experimental Results

A. Experimental System

Table III shows the circuit components in the experiment. Si-MOSFET(SPP20N60C3) is used as the power device, and the Hall current sensor (ACS724) is used in this experiment. In addition, FPGA(100 MHz) is used as a digital controller. It should be noticed that this current sensor has a 120 kHz frequency bandwidth and a 4 μs propagation delay. The current sensors inside the power module are demonstrated by installing the current sensor in series with the power devices.

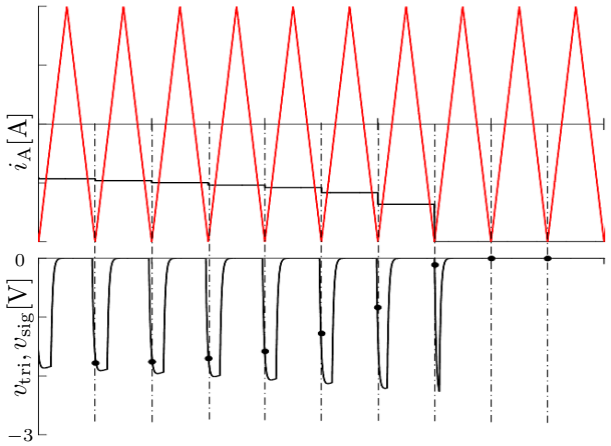

Fig. 7: PWM waveform and the output current of sensor A.

B. Experimental Results

Fig. 8 shows the experiment results with a 10 kHz carrier frequency and 50 Hz sinusoidal output current. The current sensor A was chosen, and the lower vertex of the triangle carrier is selected as the sampling point. From these experimental waveforms, it can be confirmed that the output current i_{out} is properly controlled with one current sensor in series with the power device.

Fig. 9 shows experimental results for a 20 kHz switching frequency. These circuit conditions are almost the same with the simulation condition of Fig. 6, and the experimental result corresponds to the simulation result. The calculation considering only the output delay characteristics of (1) shows that at most 66.4% of the input voltage is available, and 54% of that is used in the experiment. It means that not only the output delay characteristics but also the frequency characteristics affect the emergence of the uncontrollable region. From these results, it is difficult to realize the current control using one current sensor inside the module.

V. Alternative Edge Sampling with Pulsed Current Sampling

One current sensor can theoretically control the output current; however, realizing current control from the viewpoint of practical use is difficult. One of the main reasons is that a sampling error may occur owing to the short ON pulse. When the ON pulse period of SW1 is short, that of SW2 is longer duration. Therefore, there is a possibility that this sampling error can be avoided using two current sensors A and B. Here, it should be noticed that the sampling points are different for sensors A and B.

This paper proposes a sampling method using two current sensors in the module, and the sampling point of the current sensor is selected by the amplitude of the modulation signal v_{sig}. Fig. 10 shows the configuration diagram of the proposal method, and Fig. 11 shows the current control principle. When the modulation signal is high, the ON period of SW1 will become longer. Sensor A is selected, and the synchronous

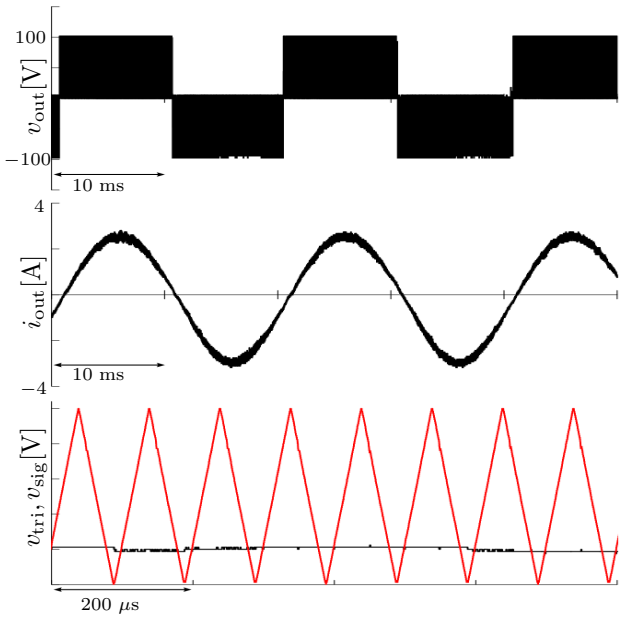

Fig. 8: Experimental waveform with sensor A for a 10-kHz switching frequency.

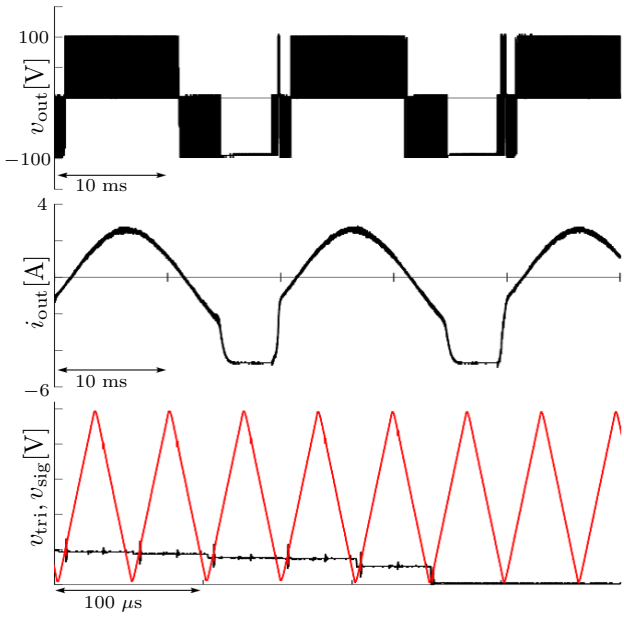

Fig. 9: Experimental waveform with sensor A for a 20-kHz switching frequency.

point is moved to the lower vertex of the carrier. In contrast, if the modulation signal is low, the synchronous point is changed to the upper vertex and sensor B is selected. This type of sampling that changes the synchronous sampling point depending on the modulation signal is already proposed [15] [16] to reduce the damage to the control of switching noises caused.

For selecting the current sensors, A and B, this paper applies hysteresis control depending on the modulation ratio, as shown in Fig. 11. As mentioned above, the modulation ratio m^* represents the maximum input voltage applied to the load as a ratio. It can be expressed in terms of PWM using the peak value of the carrier and the maximum value of the modulation signal, which is given by (7).

$$m^* = \frac{V_{\rm sig\_max}}{V_{\rm tri}} \tag{7}$$

From (3) and (7), the condition of the hysteresis threshold is given by (8). This equation indicates a threshold value for hysteresis control.

$$V_{\rm HYS} < (1 - \frac{4T_{\rm delay}}{T_{\rm carrier}}) * V_{\rm tri} \tag{8}$$

When the modulation signal $V_{\rm sig}$ becomes higher than the hysteresis threshold $V_{\rm HYS}$, the ON time of the SW1 becomes longer than that of SW2. Therefore, current sampling can obtain the correct output value using current sensor A. On the contrary, when the modulation signal $V_{\rm sig}$ is lower than $-V_{\rm HYS}$, the ON time of SW1 is shorter than that of SW2. Thus, current sampling should be done by sensor B.

$$\begin{aligned} V_{\rm sig} &> V_{\rm HYS} &&: Use\ sensor\ A \\ V_{\rm sig} &< -V_{\rm HYS} &&: Use\ sensor\ B \end{aligned}$$

Fig.12 shows the experimental result using the two sensors A and B. The experiment condition is same as the case for a 20 kHz switching frequency when current control using one current sensor is uncontrollable. It is confirmed that the output current is accurately controlled with the proposed method.

VI. Conclusion

This paper proposed a current control method using pulsed current waveforms detected by current sensors integrated in the power module. This paper assumed that the integrated sensor was installed in series with the power devices, and the simulation results verify the validity of the proposed method. A detailed analysis revealed that the uncontrollable region appeared due to the output delay and frequency characteristics of the sensor and that their influence could be formulized. The validity of the proposed method was experimentally confirmed. Therefore, it can be concluded that the output current can be controlled by the current sensor in series with the power device, and module current sensors for protection has possibility to deal with this task.

References

[1] Koya Nishimoto, Yuichi Kado, and Keiji Wada "Implementation of Decoupling Power Flow Control System in Triple Active Bridge Converter Rated at 400V, 10kW, and 20kHz," *IEEJ J. Industry Applications*, vol. 7, no. 5, pp. 410−415, 2018.

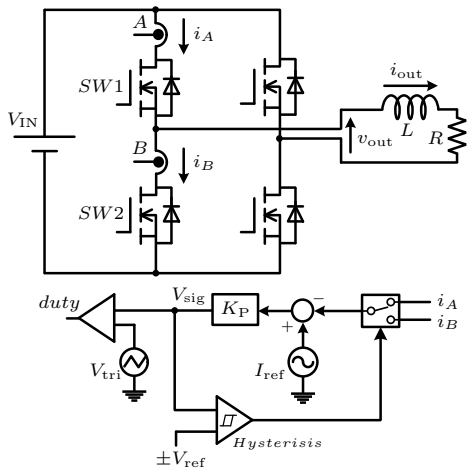

Fig. 10: Circuit and block diagram of the proposed method.

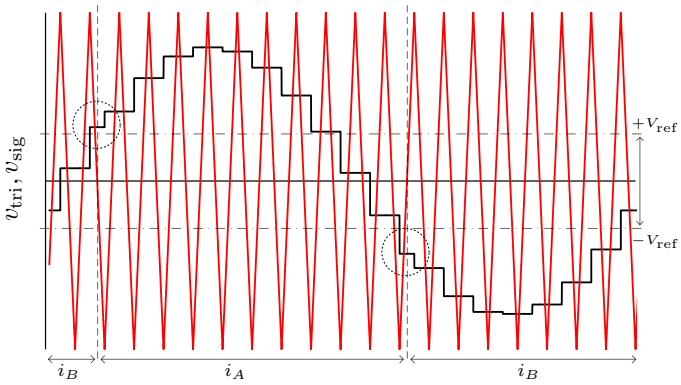

Fig. 11: Principle of alternative edge sampling method.

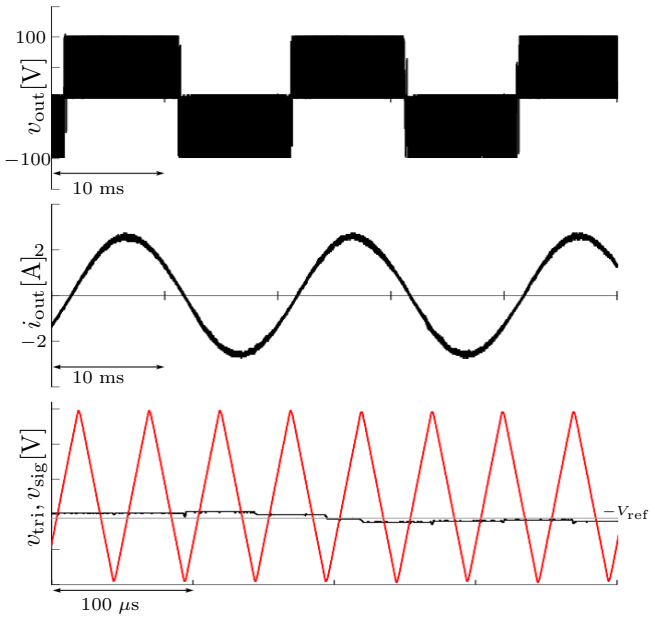

Fig. 12: Experimental waveforms for sensors A & B at 20 kHz.

[2] Aviti Mushi, Sakahisa Nagai, Hidemine Obara, and Atsuo Kawamura ”Fast and Robust Nonlinear Deadbeat Current Control for Boost Converter,” *IEEJ J. Industry Applications*, vol. 6, no. 5, pp. 311-319, 2017.

[3] Kei Matsuura, Yousuke Akama, Kodai Abe, Kiyoshi Ohishi, Hitoshi Haga, and Itaru Ando,”Fine Three-Phase Current Reconstruction based on Calculating the Phase-Shifted Voltage Reference Using Only the DC Current Sensor of an Inverter and Its Application to a PM Motor Drive,” *IEEJ J. Industry Applications*, vol.6, no.1, pp.58-65, 2017.

[4] S. M. Ahsanuzzaman and A. Prodic, “An on-chip integrated auto-tuned hybrid current-sensor for high-frequency low-power dc-dc converters,” *IEEE Applied Power Electronics Conference and Exposition - APEC*, pp. 445−450, 2015.

[5] J. Wang, Z. Shen, R. Burgos, and D. Boroyevich, “Integrated switch current sensor for short circuit protection and current control of 1.7-kV SiC MOSFET modules,” *IEEE Energy Conversion Congress and Exposition*, 2016.

[6] F. Parasiliti, R. Petrella, and M. Tursini, “Low cost phase current sensing in DSP based AC drives,” *IEEE Int. Symp. Ind. Electron.* , vol. 3, pp. 1284−1289, 1999.

[7] J. Wang, Z. Shen, R. Burgos, and D. Boroyevich, “Design of a high-bandwidth Rogowski current sensor for gate-drive short circuit protection of 1.7 kV SiC MOSFET power modules,” *IEEE Workshop on Wide Bandgap Power Devices and Applications*, 2015, pp. 104−107.

[8] T. J. Brauhn, M. Sheng, B. A. Dow, H. Nogawa, and R. D. Lorenz, “Module-integrated GMR-based current sensing for closed-loop control of a motor drive,” *IEEE Transactions on Industry Applications*, 2017, vol. 53, no. 1, pp. 222−231.

[9] S. M. Dehghan, M. Mohamadian, and A. Yazdian, “Current control of nine-switch inverter using integrated current sensors,” *International Power Engineering and Optimization Conference (PEOCO)* , 2010, pp. 95−100.

[10] J. Xu, L. Zhao, Z. Liang, and J. D. Van Wyk, “Design of an embedded bi-planar coil-based integrated current sensor for power module integration,” *IEEE Applied Power Electronics Conference and Exposition - APEC*, 2005, vol. 1, pp. 369−374.

[11] T. P. Chow, D. N. Pattanayak, E. J. Wildi, J. M. Pimbley, B. J. Baliga, and M. S. Adler, “Design of current sensors in IGBT’s,” *IEEE Trans. Electron Devices*, vol. 39, no. 11, p. 2673, 1992.

[12] Y. C. Liang, G. S. Samudra, and V. S. S. Hor, “Design of integrated current sensor for lateral IGBT power devices,” *IEEE Trans. Electron Devices*, vol. 45, no. 7, pp. 1614−1616, 1998.

[13] W. Kim, S. Luo, G. Q. Lu, and K. D. T. Ngo, “Integrated current sensor using giant magneto resistive (GMR) field detector for planar power module,” *IEEE Applied Power Electronics Conference and Exposition - APEC*, 2013, pp. 2498−2505.

[14] S. Chakrabarti, T. M. Jahns, and R. D. Lorenz, “A current reconstruction algorithm for three-phase inverters using integrated current sensors in the low-side switches,” *IEEE IAS Annu. Meet.* , vol. 2, pp. 925−932, 2003.

[15] D. M. Van De Sype, K. De Gussem, A. P. Van Den Bossche, and J. A. A. Melkebeek, “A sampling algorithm for digitally controlled boost PFC converters,” *IEEE Trans. Power Electron.*, vol. 19, no. 3, pp. 649-657, 2004.

[16] Aromhack Saysanasongkham, Masayuki Arai, Satoshi Fukumoto, Shun Takeuchi, Keiji Wada, “A Highly Reliable Digital Current Control using an Adaptive Sampling Method,” *IEEJ Journal of Industry Applications*, vol. 3, pp. 296-303, 2014.